Available online at www.sciencedirect.com
SCIENCE DIRECT®
Journal of Solid State Chemistry 177 (2004) 752–759
JOURNAL OF SOLID STATE CHEMISTRY
http://elsevier.com/locate/jssc

The new hydrides $CeNiGeH_{1.6}$ and $CeCuGeH_{1.0}$ crystallizing in the derivative hexagonal ZrBeSi-type structure

B. Chevalier,* M. Pasturel, J.-L. Bobet, F. Weill, R. Decourt, and J. Etourneau

Institut de Chimie de la Matière Condensée de Bordeaux (ICMCB), CNRS [UPR 9048], Université Bordeaux 1, Avenue du Docteur A. Schweitzer, Pessac, Cedex 33608, France

Received 17 June 2003; received in revised form 25 August 2003; accepted 3 September 2003

Abstract

The ternary germanides CeNiGe and CeCuGe absorb hydrogen in the temperature range 393–473 K. X-ray powder diffraction and transmission electron microscopy show that the hydride $CeNiGeH_{1.6(1)}$ adopts the hexagonal ZrBeSi-type whereas $CeCuGeH_{1.0(1)}$ crystallizes in a superstructure of this type. Magnetization, electrical resistivity and thermopower measurements reveal that $CeNiGeH_{1.6(1)}$ is an intermediate valence compound having a Kondo temperature $\cong 220(10)$ K smaller than that observed $\cong 600(20)$ K for CeNiGe. On the contrary, a transition from ferromagnetism to non-magnetic ordering above 1.8 K is evidenced during the hydrogenation of CeCuGe.

PACS: 61.10.Nz; 72.15.Eb; 75.30.Mb

Keywords: Hydrogenation; Cerium compounds; Intermediate valence

1. Introduction

Recently, several works devoted to the hydrogenation of ternary compounds CeMX ($M = 3$, 4, 5d transition element and $X = p$ element) crystallizing in the orthorhombic TiNiSi-type structure have shown that the resulting hydride CeMXH$_Y$ exhibits a hexagonal structure having AlB_2- or ZrBeSi-type [1–5]. In other words, the absorption of hydrogen by these intermetallics based on cerium induces a structural transition. Moreover, neutron powder diffraction performed on isostructural deuterides as $LaNiSnD_2$ [6], $TbNiSiD_{1.78}$ [7] and $TbNiGeD_{1.8}$ [8] reveals that D atoms occupy the tetrahedral [La_3Ni] or [Tb_3Ni] sites of the hexagonal ZrBeSi-type structure.

The insertion of hydrogen in these equiatomic ternary compounds CeMX induces the occurrence of interesting physical properties for the hydrides. The valence of cerium changes from intermediate valence to trivalent state during the hydrogenation of CeIrAl [4], CeNiGa [1] and CeIrGa [5]. We observed the hydride $CeAuAlH_{1.4(1)}$ presents an antiferromagnetic transition at a Néel temperature $T_N = 8.0(2)$ K more than twice greater than that determined for the Kondo antiferromagnet CeAuAl ($T_N = 3.6(2)$ K) [2]. More recently, the hydrogenation of the Kondo semiconductor ternary stannide CeNiSn leads to the hydride $CeNiSnH_{1.8(2)}$ that can be classified as a Kondo ferromagnet [3]. All these results indicate that the hydrogenation favors the localization of the 4f(Ce)-electrons.

It is well known that the physical properties of the compounds based on cerium are governed by the strength of the interaction J_{cf} between the 4f(Ce) electrons and conduction electrons [9]. The value of J_{cf} influences the competition between Kondo interaction and RKKY interaction. When the compound absorbs hydrogen, the J_{cf} value is modified and consequently this competition changes. The insertion of hydrogen in the lattice of the intermetallic leads to an expansion of the unit cell volume inducing a decrease of J_{cf} and also a modification of the density of states at the Fermi level. Hence, the hydrogenation can be considered as equivalent to an application of "negative" pressure on intermetallic. In this view, it is interesting to perform hydrogenation on intermediate valence compounds in

*Corresponding author. Fax: +33-05-56-84-27-61.
E-mail address: chevalie@icmcb.u-bordeaux.fr (B. Chevalier).

0022-4596/$ - see front matter © 2003 Elsevier Inc. All rights reserved.
doi:10.1016/j.jssc.2003.09.003

order to discover new materials presenting magnetic ordering influenced by Kondo effect, superconducting properties…

The aim of the present work is to study the response of CeNiGe exposed to hydrogen. This compound crystallizes in the orthorhombic TiNiSi-type structure and is considered as an intermediate valence system having a high ($\gg 300$ K) Kondo temperature [10–13]. For comparison, the study concerning the hydrogenation of CeCuGe which shows a ferromagnetic transition at $T_C = 10.2$ K is also presented [14]. The new hydrides $CeNiGeH_{1.6(1)}$ and $CeCuGeH_{1.0(1)}$ have been investigated by X-ray powder diffraction, transmission electron microscopy (TEM) and magnetization, electrical resistivity and thermopower measurements.

2. Experimental details

Polycrystalline CeNiGe and CeCuGe samples were synthesized by arc-melting a stoichiometric mixture of pure elements (purity above 99.9%) in a high-purity argon atmosphere. Then, the samples were turned and remelted several times to ensure homogeneity. An annealing treatment was performed in evacuated quartz tube for 1 month at 1073 and 973 K, respectively, for CeNiGe and CeCuGe.

Hydrogen absorption experiments were performed using the apparatus described previously [15]. An ingot (mass of around 1 g) of an annealed sample was heated under vacuum at 473 K for 12 h and then exposed to 5 MPa of hydrogen gas at the same temperature. The amount of H absorbed was determined volumetrically by monitoring pressure changes in a calibrated volume. The hydrogen absorption and desorption kinetics of CeNiGe and CeCuGe were measured using an automated Sievert's-type apparatus (HERA) with sample of about 500 mg.

X-ray powder diffraction with the use of a Philips 1050-diffractometer (Bragg–Brentano geometry, Cu$K\alpha$ radiation, diffracted-beam graphite monochromator) was applied for the characterization of the structural type and for the phase identification of the samples before and after hydrogenation. The crystal structures of CeNiGe and CeCuGe and their hydrides were refined by the Rietveld profile method by the Fullprof program [16]. For electron microscopy experiments (JEOL 2000FX), parts of the hydride sample were crushed in ethanol in an agate mortar and the small fragments were placed on a copper grid covered with an amorphous holey carbon film.

Magnetization measurements were performed using a Superconducting Quantum Interference Device magnetometer in the temperature range 1.8–300 K and applied fields up to $5T$. Electrical resistivity was carried out above 4.2 K on a polycrystalline sample using standard dc four probe measurements. For this investigation, the hydride was compacted at room temperature (compactness $\cong 80\%$) in order to form a pellet (diameter = 6 mm and thickness = 3 mm) and then heated for 2 days at 473 K under hydrogen pressure (5 MPa). Thermoelectric power measurements were performed on the same pellet using a dynamic method. Details of the cell used and measurement methods have been described previously [17].

3. Results and discussion

Under the experimental conditions described above ($T = 473$ K and $P(H_2) = 5$ MPa), CeNiGe and CeCuGe absorb hydrogen. The amount of H atom inserted is 1.6(1) and 1.0(1) per CeNiGe and CeCuGe formula, respectively. The hydrides formed are stable in air and show a metallic aspect. Also, the H absorption induces a decrepitating in small grains of the pure starting ingots.

Fig. 1 presents selected first hydrogen absorption performed at various $P(H_2)$ pressure on these two compounds. At low pressure (0.2 MPa), the kinetic of the hydrogen absorption is very slow; for instance the hydride $CeNiGeH_{1.6(1)}$ is obtained after 13 h of exposure (Fig. 1(a)). On the contrary, an increase of $P(H_2) = 2$ MPa induces a rapid absorption. $CeCuGeH_{1.0(1)}$ is prepared after 4 min of exposure. We note also that CeNiGe absorbs more hydrogen than CeCuGe. This result agrees with those reported previously on $LaNi_{5-x}Cu_x$ system [18,19] showing a decrease of the hydrogen solubility with increasing copper content.

3.1. Structural properties

3.1.1. CeNiGe and $CeNiGeH_{1.6(1)}$

X-ray powder diffraction performed on CeNiGe confirms that this ternary germanide crystallizes in the orthorhombic TiNiSi-type structure (space group *Pnma*; No 62). The refined unit cell parameters, given in Table 1, are in agreement with those determined previously [10]. In this structure, Ce, Ni and Ge occupy the sites 4*c* ($-0.004(1)\frac{1}{4}0.2084(4)$), 4*c* ($0.202(1)\frac{1}{4}0.581(1)$) and 4*c* ($0.803(1)\frac{1}{4}0.5955(9)$). (Standard deviations in the data of the least-significant digits are given in brackets throughout the paper.)

The hydrogenation of CeNiGe induces a structural transition (Fig. 2) (the crystallization state of this hydride is not so good because the hydrogenation induces a reconstruction of the crystal structure). X-ray powder pattern of $CeNiGeH_{1.6(1)}$ is indexed on the basis of the hexagonal ZrBeSi-type structure (space group $P6_3/mmc$; No 194) (Table 1): Ce atoms occupying the 2*a* site (000) whereas Ni and Ge atoms are located, respectively, on the 2*c* site ($\frac{1}{3}\frac{2}{3}\frac{1}{4}$) and 2*d* site ($\frac{1}{3}\frac{2}{3}\frac{3}{4}$) (*reliability factors:* $R_F = 0.063$; $R_p = 0.121$ *and*

$R_{wp} = 0.160$). Similar structural transition orthorhombic TiNiSi-type → hexagonal ZrBeSi-type was observed previously during the hydrogenation of the ternary germanide TbNiGe [8]. In both structures types, Ni- and Ge atoms form a hexagonal network, which are close packed, and regular in CeNiGe and $CeNiGeH_{1.6(1)}$ [20].

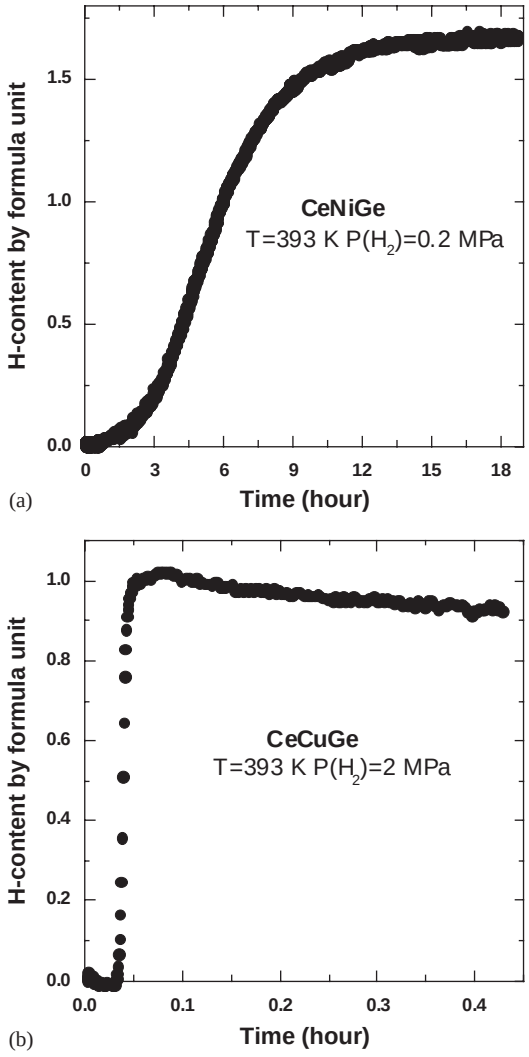

Fig. 1. First hydrogen absorption at 393 K for (a) CeNiGe ($P(H_2) = 0.2$ MPa), and (b) CeCuGe ($P(H_2) = 2$ MPa).

To confirm the crystal symmetry of $CeNiGeH_{1.6(1)}$, transmission electron microscopy has been performed. Selected-area electron diffraction patterns along the zone directions [0−10] and [1−10] are shown in Figs. 3(a) and (b). Comparison of these two patterns indicates that for (*hhl*) reflections a condition for extinction exists: $h\,h\,l$ with $l = 2n + 1$. This agrees with the presence of a *c*-type glide plane as for the ZrBeSi-type structure (space group $P6_3/mmc$).

The formation of $CeNiGeH_{1.6(1)}$ hydride is accompanied by a large increase ($\cong 11.6\%$) of the unit cell volume per mol (Table 1). Also, the interatomic distances $d_{Ce-NiorGe}$ existing in the hydride are greater than those observed in CeNiGe (Table 2). These steric considerations suggest that the valence state of the cerium could be modified during the hydrogenation.

3.1.2. *CeCuGe and $CeCuGeH_{1.0(1)}$*

Controversy exists concerning the structural properties of the ternary germanide CeCuGe. Yang et al. [14]

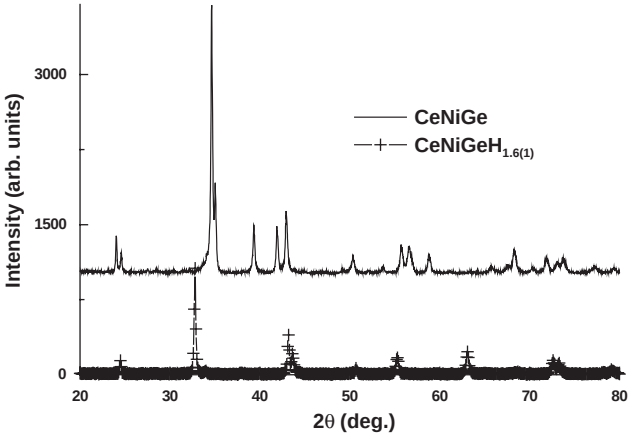

Fig. 2. X-ray powder diffraction pattern (Cu*K*α radiation) of CeNiGe and its hydride $CeNiGeH_{1.6(1)}$.

Table 1
Crystallographic data relative to the ternary germanides CeNiGe and CeCuGe and their hydrides. (V_m represents the unit cell volume per mol)

Compound	Symmetry	Type structure	Unit cell parameters				Reference
			a (Å)	*b* (Å)	*c* (Å)	V_m (Å)^3	
CeNiGe	Orthorhombic	TiNiSi	7.2418(3)	4.3078(2)	7.2408(4)	56.47(4)	[10]
CeNiGe	Orthorhombic	TiNiSi	7.2469(5)	4.3083(3)	7.2379(6)	56.50(5)	[a]
$CeNiGeH_{1.6(1)}$	Hexagonal	ZrBeSi	4.190(1)		8.293(2)	63.04(2)	[a]
CeCuGe	Hexagonal	ZrBeSi	4.311		7.933	63.84	[14]
CeCuGe	Hexagonal	AlB_2	4.308(2)		3.966(2)	63.74	[21]
CeCuGe	Hexagonal	ZrBeSi	4.302(1)		7.919(2)	63.46(2)	[a]
$CeCuGeH_{1.0(1)}$[b]	Hexagonal	ZrBeSi	4.244(1)		8.311(2)	64.82(2)	[a]

[a] This work.
[b] Average crystal structure.

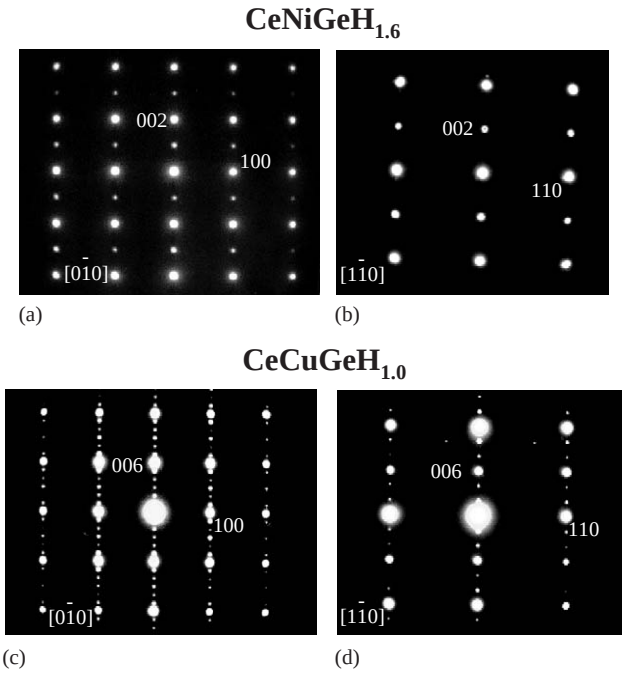

Fig. 3. Selected-area electron diffraction patterns of $CeNiGeH1_{.6(1)}$ and $CeCuGeH_{1.0(1)}$ along the [0−10] (a,c), and [1−10] (b,d) directions.

Table 2
Selected interatomic distances (Å) in CeNiGe and $CeNiGeH_{1.6(1)}$

CeNiGe	$CeNiGeH_{1.6(1)}$
Ce-2 Ce 3.673	Ce-6 Ce 4.190
Ce-2 Ce 3.707	Ce-2 Ce 4.147
Ce-2 Ce 4.308	
Ce-2 Ce 4.739	
Ce- Ni 2.988	Ce-12 (Ni,Ge) 3.186
Ce-2 Ni 3.004	
Ce-Ni 3.082	
Ce-2 Ni 3.206	
Ce-2 Ge 2.963	
Ce-Ge 3.129	
Ce-Ge 3.132	
Ce-2 Ge 3.163	

indicate that this compound adopts the hexagonal ZrBeSi-type whereas Iandelli [21] points out a hexagonal AlB_2-type. The present investigation by X-ray powder diffraction confirms the results of Yang et al. (Table 1). The occurrence of an ordered Cu, Ge-network (ZrBeSi-type) is strongly dependent on the temperature and duration of the annealing treatment.

For $CeCuGeH_{1.0(1)}$, the typical electron diffraction patterns obtained for the [0−10] and [1−10] zone axis are quite different from those observed for $CeNiGeH_{1.6(1)}$ (Figs. 3(c) and (d)). Weak superstructure reflections appear along 0 0 1 direction of its reciprocal lattice which cannot be indexed in the primitive hexagonal ZrBeSi cell. This investigation reveals that the [001] direction periodicity in $CeCuGeH_{1.0(1)}$ hydride is three times that of the ZrBeSi cell. The existence of this superstructure can be explained by the presence of an order in the partial occupancy of the crystallographic site ($\frac{1}{3}\frac{2}{3}\cong 0.4365$ in the ZrBeSi-type) [6,7]. If this site is fully occupied, the resulting hydride would contain two H atoms per formula unit but in the present study only 1.0(1) H atoms are inserted in the CeCuGe cell. In other words, the occurrence of the superstructure of $CeCuGeH_{1.0(1)}$ results from an ordering of the hydrogen occupation. The investigation of this hydride (deuteride) by neutron powder diffraction is considered in order to determine its crystal structure. In the following, the structural properties of $CeCuGeH_{1.0(1)}$ on the basis of its average crystal structure (ZrBeSi-type) as determined by X-ray powder diffraction is discussed (Fig. 4). In this case, the hydride exhibits a good crystallization state.

The hydrogenation of CeCuGe causes a drastic anisotropic expansion of the unit cell (Table 1): the *a*-parameter decreases weakly (−1.3%) whereas the *c*-parameter increases strongly (+5.0%). This last increase is probably connected to the insertion of H atoms in the 4*f* site ($\frac{1}{3}\frac{2}{3}\cong 0.4365$), which influences the expansion of the *c*-parameter [6,7]. The unit cell volume per mol V_m increases ($\cong 2.1\%$) weakly during the hydrogenation so that, the valence state of Ce atoms should not be influenced by this treatment.

It is interesting to compare the unit cell parameters determined for $CeNiGeH_{1.6(1)}$ and $CeCuGeH_{1.0(1)}$ (Table 1). As the metallic radius of copper (1.278 Å) is greater than that of nickel (1.246 Å), the *a*- and *c*-parameters of $CeCuGeH_{1.0(1)}$ are much higher. This fact is confirmed by the evolution of the $d_{Ce-(NiorCu),Ge}$ interatomic distances given in Tables 2 and 3.

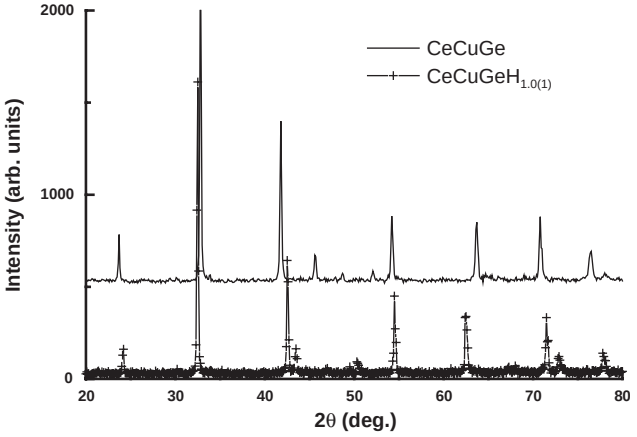

Fig. 4. X-ray powder diffraction pattern (Cu*K*α radiation) of CeCuGe and its hydride $CeCuGeH_{1.0(1)}$.

Table 3
Selected interatomic distances (Å) in CeCuGe and $CeCuGeH_{1.0(1)}$

CeCuGe	$CeCuGeH_{1.0(1)}$
Ce-6 Ce 4.302	Ce-6 Ce 4.244
Ce-2 Ce 3.960	Ce-2 Ce 4.156
Ce-12 (Cu,Ge) 3.176	Ce-12 (Cu,Ge) 3.213

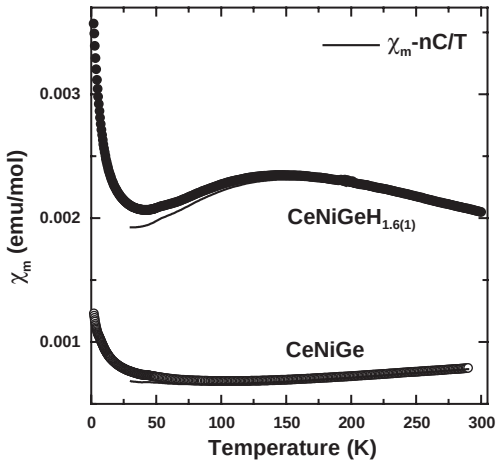

Fig. 5. Temperature dependence of the magnetic susceptibility χ_m, measured with an applied field $\mu_0 H = 4$ T, of germanide CeNiGe and its hydride $CeNiGeH_{1.6(1)}$. Solid lines show the fit to calculated χ_m, using $\chi_m = \chi_m(0) + nC/T$ (see text).

3.2. Magnetic and electrical properties

3.2.1. CeNiGe and $CeNiGeH_{1.6(1)}$

Fig. 5 presents the temperature dependence of the magnetic susceptibility χ_m of CeNiGe and its hydride. An appreciable increase in the χ_m value of the hydride is observed relative to that of CeNiGe.

Above 60 K, χ_m of CeNiGe increases slowly with the temperature (the upturn below 60 K is probably attributed to the presence of traces ($\cong 0.1\%$ in weight) of magnetic impurity phases as Ce_2O_3). This behavior characterizes a nearly Pauli-paramagnet indicating that the 4*f*(Ce)-electrons are strongly hybridized with those of the conduction band [11,12]. The curve $\chi_m = f(T)$ concerning the hydride $CeNiGeH_{1.6(1)}$ shows a broad maximum centered around 130(5) K. Such a behavior is commonly observed in intermediate valence systems [22]. The experimental temperature dependence of χ_m can be expressed in terms of a characteristic temperature T_K related to Kondo-type fluctuations. In this scheme relative to valence-fluctuating compounds, T_K is defined, below the broad maximum, as $T_K = C/2\chi_m(0)$ where $C = 0.807$ emu K/mol is the Curie constant for free Ce^{3+} ions and $\chi_m(0)$ is the magnetic susceptibility at $T = 0$ K. (This model, offered by Lawrence et al. [22], forecasts that the $\chi_m = f(T)$ curve exhibits a maximum around $T = T_K/2$.) $\chi_m(0)$ is obtained by fitting of χ_m at low temperatures according to: $\chi_m = \chi_m(0) + nC/T$ (Fig. 5) where n is the proportion of stable Ce^{3+} moments composing the traces of magnetic impurities. For the hydride $CeNiGeH_{1.6(1)}$, we obtain the following values: $n = 6.5(5)10^{-3}$ Ce^{3+} ions/mol, $\chi_m(0) = 1.83(5)10^{-3}$ emu/mol and $T_K = 220(10)$ K. From this T_K value, it is expected that $\chi_m = f(T)$ possesses a broad maximum near $T_K/2 = 110(10)$ K which is comparable with the experimental value of 130(5) K. A similar calculation performed on CeNiGe gives $T_K = 600(20)$ K. It can be concluded that the insertion of a H atom into CeNiGe induces a decrease of the mixing between 4*f*(Ce) and conduction electrons but the resulting hydride may be considered as a valence-fluctuating compound.

This assumption is confirmed by the temperature dependence of the reduced electrical resistivity of CeNiGe and $CeNiGeH_{1.6(1)}$ (Fig. 6). For CeNiGe, the resistivity decreases practically linearly with the temperature between 270 and 50 K and then takes a constant value below 15 K. This behavior characterizes a non-magnetic metal indicating that the 4*f*(Ce)-electrons are practically delocalized in CeNiGe. A different feature appears for $CeNiGeH_{1.6(1)}$. In this case, the curve $\rho(T)/\rho(270\,\mathrm{K}) = f(T)$ shows a large maximum around 120(5) K, associated with a steep decrease below this temperature and a smoother one above. This variation is very similar to that observed in $Ce(Pt_{1-x}Ni_x)Si$ $(0.5 \leqslant x \leqslant 1)$ and $CeNi_2(Ge_{1-x}Si_x)_2$ $(0.1 \leqslant x \leqslant 1)$ intermediate valence systems [23,24]. It is noted that the temperature (120(5) K) where the $\rho(T)/\rho(270\,\mathrm{K}) = f(T)$ curve goes through a maximum is close (130(5) K) to that of the $\chi_m = f(T)$ exhibits also a maximum. This agrees with the interpretation that the resistivity peak is due to a spin-scattering mechanism in the intermediate valence regime [23].

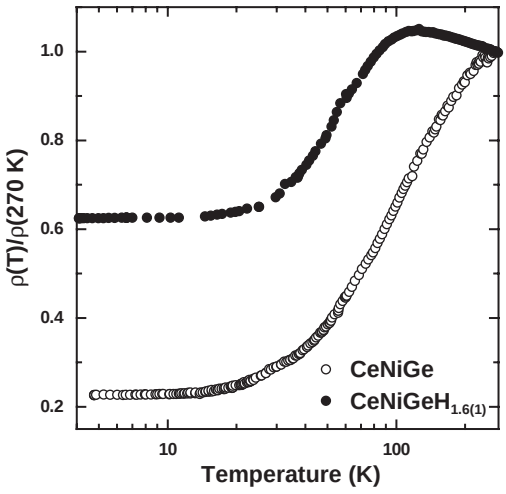

Fig. 6. Reduced electrical resistivity as a function of log T for CeNiGe and its hydride $CeNiGeH_{1.6(1)}$.

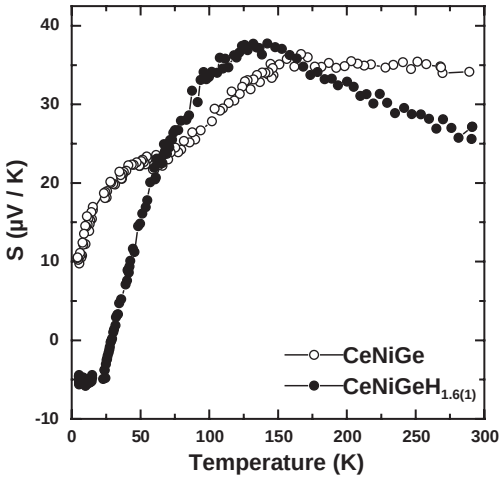

Fig. 7. Temperature dependence of the thermopower of CeNiGe and its hydride.

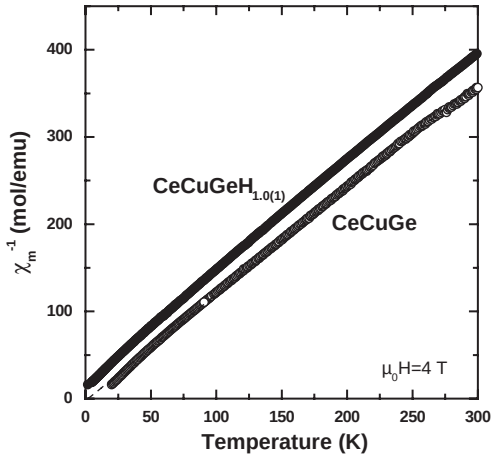

Fig. 8. Temperature dependence of the reciprocal magnetic susceptibility χ_m^{-1}, measured with an applied field $\mu_0 H = 4\,\mathrm{T}$, of germanide CeCuGe and its hydride $CeCuGeH_{1.0(1)}$. Dashed lines show the fit to calculated χ_m^{-1} with Curie–Weiss law.

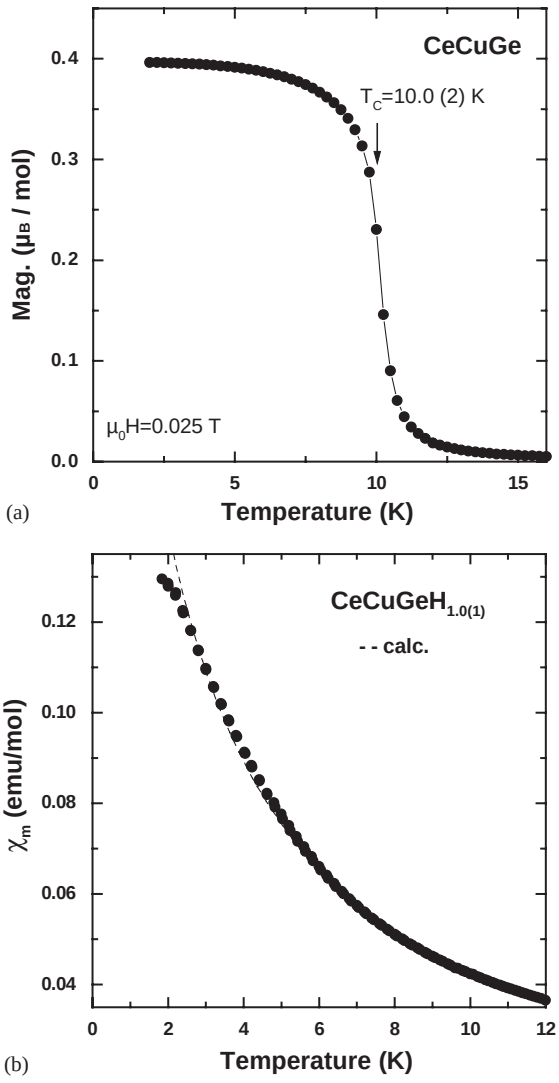

Fig. 9. Temperature dependence at low temperature of the magnetization of CeCuGe (a), and of the magnetic susceptibility of $CeCuGeH_{1.0(1)}$ (b).

Among the ternary germanides CeMGe with M = Ni, Pd and Pt, CeNiGe is known to have a much larger thermopower S at room temperature (47 μV/K) than a normal metal [13]. This behavior is connected to the intermediate valence state of the cerium in this compound (very high Kondo temperature). Fig. 7 compares the temperature dependence of the thermopower of CeNiGe and its hydride. Below 300 K, S for CeNiGe is always positive implying that the dominant carriers are holes. Between 300 and 150 K, S increases very slowly from 34(2) to 36(2) μV/K then decreases and exhibits a shoulder around 50–60 K. These data agree with those previously reported [13], although the reported maximum S value is 47 μV/K. This difference is certainly due to the difference in the sample preparation (as-cast or annealed). The $S = f(T)$ curve of CeNiGe resembles that observed for $CePd_3$ which is well known as a canonical intermediate valence compound [25,26]. The curve $S = f(T)$ relative to the hydride $CeNiGeH_{1.6(1)}$ shows a clear different behavior. It is mainly characterized by the existence of two extremes: a positive maximum of about 38(2) μV/K near 125(5) K and a weakly pronounced negative −5 μV/K around 15(2) K. There is also a change in sign at $T = 28(2)$ K. Similar change of sign has been observed for nearly trivalent cerium-based compounds as $CeCu_2Si_2$, $CeAl_2$ and $CeAl_3$ [25]. On such compounds, a positive maximum appears in the $S = f(T)$ curve at around $T = T_K/2 = 110(10)$ K (close to the experimental value of 125(5) K (Fig. 7)) due to the scattering of conduction electrons by the Kondo resonance state which is located just above the Fermi level [25].

The two curves $S = f(T)$ observed presently for CeNiGe and its hydride, are characteristic of many

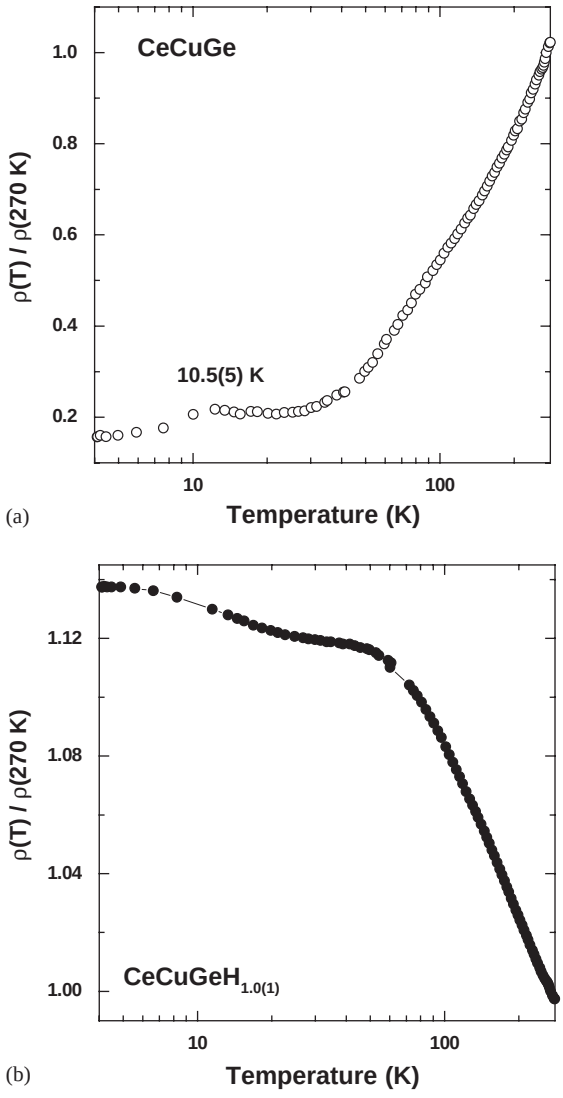

Fig. 10. Reduced electrical resistivity as a function of $\log T$ for CeCuGe (a), and $CeCuGeH_{10(1)}$ (b).

compounds based on cerium. These thermopower behaviors can be compared to those described recently by Link et al. [27], which have applied isostatic pressure on the ternary silicide $CePd_2Si_2$. Without pressure, S of this last compound exhibits at low temperature a negative peak followed by a broad positive contribution with increasing temperature. On the contrary, under a pressure of 5.6 GPa the curve $S = f(T)$ is always positive showing a shoulder at low temperature and a clear peak at high temperature. The transition between these two behaviors is explained by the sequence nearly trivalent cerium → intermediate valence cerium induced by the pressure. An opposite sequence is detected here by insertion of H atom into CeNiGe. This result confirms that in this case, the hydrogenation can be considered as an application of "negative" pressure on compounds based on cerium.

3.2.2. *CeCuGe and $CeCuGeH_{1.0(1)}$*

In the paramagnetic range, the magnetic susceptibility of these compounds follows a Curie–Weiss law $\chi_m^{-1} = (T - \theta_p)/C_m$ (Fig. 8). The effective magnetic moment $\mu_{eff} = (8C_m)^{1/2}$ and the Curie paramagnetic temperature θ_p are, respectively, equal to 2.56(5) μ_B/Ce-mol and 2(1) K for the ternary germanide CeCuGe and 2.50(5) μ_B/Ce-mol and –14(1) K for the hydride. The μ_{eff} values are in agreement with that calculated for a free Ce^{3+} ion (2.54 μ_B/Ce-mol). We note that the θ_p temperature changes in sign after insertion of *H*atom in CeCuGe. This suggests that the magnetic ordering appearing for CeCuGe is modified after hydrogenation.

Fig. 9(a) presents the temperature dependence of the magnetization of CeCuGe cooled in an applied magnetic field $\mu_0 H = 0.025$ T. The strong increase of the magnetization versus temperature characterizes the occurrence of ferromagnetic ordering. The transition temperature T_C, determined from the inflection point of the magnetization curve $M = f(T)$ equals to 10.0(2) K. This value agrees with that determined previously (10.2 K) using specific heat measurements [14]. On the contrary, no magnetic ordering can be clearly detected above 1.8 K from the curve $\chi_m = f(T)$ giving the temperature dependence of the magnetic susceptibility of the hydride $CeCuGeH_{1.0(1)}$ (Fig. 9(b)). In the temperature range 1.8–12 K, χ_m of this hydride can be fitted by a Curie–Weiss law having as parameters $\mu_{eff} = 1.98(5)\ \mu_B$/Ce-mol and $\theta_p = 1.5(5)$ K.

The absence of magnetic ordering for $CeCuGeH_{1.0(1)}$ is evidenced by electrical resistivity measurements (Fig. 10). The temperature dependence of electrical resistivity of CeCuGe shows a sharp decrease at 10.5(5) K. The last behavior is attributed to the ferromagnetic ordering observed at $T_C = 10.0(2)$ K by magnetization measurements. The curve $\rho(T)/\rho(270\,K) = f(T)$ relative to $CeCuGeH_{1.0(1)}$ hydride exhibits a different feature. Starting from 270 K, ρ first increases with decreasing temperature and is almost linear in log T between 270 and 100 K (this behavior characterizes the influence of CEF effect [28]). Then, a shoulder appears around 60 K and finally ρ increases slightly below 15 K. At low temperature, no anomaly ascribed to the occurrence of a magnetic ordering can be detected. The lack of coherence observed below 15 K (increase of ρ) may be explained by possible random magnetic interactions induced by the distribution between *H*atom and vacancies in this hydride.

4. Conclusion

The hydrogenation process of the ternary germanides CeNiGe and CeCuGe is reported for the first time. The hydrogen insertion into the CeNiGe lattice induces both a structural transition from orthorhombic TiNiSi-type

to hexagonal ZrBeSi-type and a decrease of the Kondo temperature from 600(20) to 220(10) K. The expansion of the unit cell volume per mol ($\cong$11.6%) smaller than that observed during the hydrogenation of CeNiAl ($\cong$24%) [29] or CeNiGa ($\cong$16–20%) [1] is not sufficient to drive the valence of the Ce atom toward the trivalent state. In contrast, the hydride $CeCuGeH_{1.0(1)}$ presents a derivative structure of the ZrBeSi-type. In this case, the hydrogenation suppresses the magnetic ordering.

References

[1] B. Chevalier, J.-L. Bobet, E. Gaudin, M. Pasturel, J. Etourneau, J. Solid State Chem. 168 (2002) 28.
[2] B. Chevalier, J.-L. Bobet, M.L. Kahn, F. Weill, J. Etourneau, J. Alloys Compds. 334 (2002) 20.
[3] B. Chevalier, J.-L. Bobet, M. Pasturel, E. Bauer, F. Weill, R. Decourt, J. Etourneau, Chem. Mater. 15 (2003) 2181.
[4] S.K. Malik, P. Raj, A. Sathyamoorthy, K. Shashikala, N. Harish Kumar, L. Menon, Phys. Rev. B 63 (2001) 172418.
[5] P. Raj, A. Sathyamoorthy, K. Shashikala, C.R. Venkateswara Rao, S.K. Malik, Solid State Commun. 120 (2001) 375.
[6] V.A. Yartys, T. Olavesen, B.C. Hauback, H. Fjellvag, H.W. Brinks, J. Alloys Compds. 330–332 (2002) 141.
[7] H.W. Brinks, V.A. Yartys, B.C. Hauback, J. Alloys Compds. 322 (2001) 160.
[8] H.W. Brinks, B.C. Hauback, Int. Symp. on Metal Hydrogen Systems, MH 2002, Annecy (France) 2002, p. 137.
[9] G.R. Stewart, Rev. Mod. Phys. 73 (2001) 797.
[10] P. Salamakha, M. Konyk, O. Sologub, O. Bodak, J. Alloys Compds. 236 (1996) 206.
[11] J.P. Kuang, H.J. Cui, J.Y. Li, F.M. Yang, H. Nakotte, E. Brück, F.R. De Boer, J. Magn. Magn. Mater. 104–107 (1992) 1475.
[12] B. Chevalier, J. Etourneau, J. Magn. Magn. Mater. 196–197 (1999) 880.
[13] J. Sakurai, D. Huo, D. Kato, T. Kuwai, Y. Isikawa, K. Mori, Physica B 281–282 (2000) 98.
[14] Fuming Yang, J.P. Kuang, Jingyuan Li, E. Brück, H. Nakotte, F.R. de Boer, Xiucheng Wu, Zhenxiao Li, Yupeng Wang, J. Appl. Phys. 69(8) (1991) 4705.
[15] J.-L. Bobet, S. Pechev, B. Chevalier, B. Darriet, J. Alloys Compds. 267 (1998) 136.
[16] J. Rodriguez-Carvajal, Powder diffraction, in: Satellite Meeting of the 15th Congress of IUCr, Toulouse, 1990, p. 127.
[17] P. Dordor, E. Marquestaut, G. Villeneuve, Rev. Phys. Appl. 15 (1980) 1607.
[18] A. Pasturel, F. Liautaud, C. Colinet, C. Allibert, A. Percheron-Guégan, J.C. Achard, J. Less-Common Met. 96 (1984) 93.
[19] D.V. Schur, S.Yu. Zaginaichenko, Z.A. Matysina, I. Smityukh, V.K. Pishuk, J. Alloys Compds. 330–332 (2002) 70.
[20] R.–D. Hoffmann, R. Pöttgen, Z. Kristallogr. 216 (2001) 127.
[21] A. Iandelli, J. Alloys Compds. 198 (1993) 141.
[22] J.M. Lawrence, P.S. Riseborough, R.D. Parks, Rep. Prog. Phys. 44 (1981) 1.
[23] W.H. Lee, H.C. Ku, R.N. Shelton, Phys. Rev. B 36 (1987) 5739.
[24] G. Knebel, M. Brando, J. Hemberger, M. Nicklas, W. Trinkl, A. Loidl, Phys. Rev. B 59 (1999) 12390.
[25] D. Jaccard, J. Sierro, in: P. Wachter, H. Boppart (Eds.), Valence Instabilities, North-Holland, Amsterdam, 1982, p. 409.
[26] M. Houshiar, D.T. Adroja, B.D. Rainford, Physica B 223–224 (1996) 268.
[27] P. Link, D. Jaccard, P. Lejay, Physica B 225 (1996) 207.
[28] B. Cornut, B. Coqblin, Phys. Rev. B 5 (1972) 4541.
[29] J.-L. Bobet, B. Chevalier, B. Darriet, M. Nakhl, F. Weill, J. Etourneau, J. Alloys Compds. 317–318 (2001) 67.